JPET Fast Forward. Published on March 4, 2019 as DOI: 10.1124/jpet.118.252965
This article has not been copyedited and formatted. The final version may differ from this version.

1.0 Title Page

Reduced tolerance and asymmetrical cross-tolerance to effects of the indole quinuclidinone analogue PNR-4-20, a G protein biased CB_1R agonist in mice: comparisons with Δ^9-THC and JWH-018

Benjamin M. Ford[a], Christian V. Cabanlong[a], Sherrica Tai[a], Lirit N. Franks[a], Narsimha R. Penthala[b], Peter A. Crooks[b], Paul L. Prather[a] and William E. Fantegrossi[a]*

Author affiliations:

[a]Department of Pharmacology and Toxicology, College of Medicine, University of Arkansas for Medical Sciences, 4301 West Markham Street, Little Rock, AR 72205

[b]Department of Pharmaceutical Sciences, College of Pharmacy, University of Arkansas for Medical Sciences, 4301 West Markham Street, Little Rock, AR 72205, USA.

2.0 Running Title Page

a. PNR-4-20 produces less tolerance than other CB_1R agonists

b. **Corresponding Author**
William E. Fantegrossi
Department of Pharmacology and Toxicology
College of Medicine, University of Arkansas for Medical Sciences
4301 West Markham Street
Little Rock, AR 72205
Phone: 686-8645
Fax: 686-8970
email: wefantegrossi@uams.edu

c. 18 text pages
3 reference pages (51 references)
5 figures
3 tables
Abstract (245 words)
Introduction (723 words, excluding citations)
Discussion (1426 words, excluding citations)

d. **Abbreviations**
CB1 cannabinoid receptors (CB_1Rs)
CB2 cannabinoid receptors (CB_2Rs)
Indole quinuclidinone (IQD)
Δ^9-tetrahydrocannabinol (Δ^9-THC)

e. **Recommended section assignment**
Behavioral Pharmacology

JPET Fast Forward. Published on March 4, 2019 as DOI: 10.1124/jpet.118.252965
This article has not been copyedited and formatted. The final version may differ from this version.

3.0 Abstract

Most cannabinoid CB_1 receptor (CB_1R) agonists signal through both G protein-dependent and –independent pathways in an unbiased manner. Recruitment of β-arrestin 2 desensitizes and internalizes receptors, producing tolerance which limits therapeutic utility of cannabinoids for chronic conditions. We developed the indole quinuclidinone (IQD) analogue PNR-4-20 as a novel G protein-biased agonist at CB_1Rs, and the present studies determine if repeated administration of PNR-4-20 produces lesser tolerance to *in vivo* effects as compared to unbiased CB_1R agonists Δ^9-THC and JWH-018. Adult male NIH Swiss mice were administered comparable doses of PNR-4-20 (100 mg/kg), Δ^9-THC (30 mg/kg) or JWH-018 (3 mg/kg) once per day for 5 consecutive days in order to determine tolerance development to hypothermic, antinociceptive and cataleptic effects. Persistence of tolerance was then determined after a drug abstinence period. We found that unbiased CB_1R agonists Δ^9-THC and JWH-018 produced similar tolerance to these effects, but lesser tolerance was observed with PNR-4-20 for hypothermic and cataleptic effects. Tolerance to the effects of PNR-4-20 completely recovered after drug abstinence, while residual tolerance was always observed with unbiased CB_1R agonists. Repeated treatment with PNR-4-20 and Δ^9-THC produced asymmetrical cross-tolerance to hypothermic effects. Importantly, binding studies suggest PNR-4-20 produced significantly less downregulation of CB_1Rs relative to Δ^9-THC in hypothalamus and thalamus of chronically treated mice. These studies suggest that the G protein-biased CB_1R agonist PNR-4-20 produces significantly less tolerance than unbiased cannabinoid agonists, and that the IQD analogues should be investigated further as a novel molecular scaffold for development of new therapeutics.

5.0 Introduction

Investigation of CB_1 (CB_1Rs) and CB_2 (CB_2Rs) cannabinoid receptors has identified numerous ligands with therapeutic potential (Eisenstein, 2015). Cannabinoids like Δ^9-tetrahydrocannabinol (Δ^9-THC) have been reported to alleviate cachexia (Cressey, 2015; Reuter and Martin, 2016), chronic pain (Berlach et al., 2006; Lynch and Ware, 2015), anorexia (Verty et al., 2011), and Dravet syndrome (Devinsky et al., 2017; Rosenberg et al., 2017). Numerous states and municipalities within the US have endorsed the medical use of cannabis, and many laboratories have demonstrated the therapeutic potential of both phytocannabinoids and synthetic cannabinoids (Price et al., 2005; Horswill et al., 2007; Piscitelli et al., 2012; Madadi et al., 2013), but few such ligands have undergone clinical trials or achieved FDA approval as medications. Currently, two Δ^9-THC analogues, dronabinol and nabilone, are indicated for chemotherapy-induced nausea and vomiting, but are not highly utilized treatments in most clinical settings (Muramatsu et al., 2013; Volkow et al., 2014; Pergolizzi et al., 2017). As observed in both clinical studies and in incidences of recreational abuse, CB_1R agonists like Δ^9-THC produce a psychotomimetic “high” following acute use, and can produce adverse effects such as tolerance, dependence and withdrawal following chronic use (Ware et al., 2008; Weinstein and Gorelick, 2011; Cooper et al., 2013; Maida and Daeninck, 2016). Overall, development of cannabinoid ligands devoid of these adverse effects will likely be essential for the widespread acceptability of cannabimimetics as mainstream therapeutics.

In this regard, the biological effects of cannabinoid ligands are transduced through intracellular signaling mechanisms initiated by binding to cannabinoid CB_1Rs and CB_2Rs (Matsuda et al., 1990; Howlett et al., 2002). Interestingly, CB_1Rs and CB_2Rs both bind a structurally diverse range of cannabinoid ligands with varying efficacies, including endogenously produced eicosanoids (*e.g.*, anandamide and 2-archidinoylglycerol), plant derived phytocannabinoids (*e.g.*, Δ^9-THC) and synthetic cannabinoids (*e.g.*, CP 55,940, WIN 55-212-2, JWH-018) (Pertwee, 1997; Pertwee, 2006). When unbiased agonist ligands bind these receptors,

a convergence of several signaling processes, both G protein-dependent and –independent, are initiated. For CB_1Rs, G protein-independent signaling has been shown to hinder therapeutically-relevant G protein signaling *via* β-arrestin 2 mediated desensitization and downregulation of the receptor (Raehal and Bohn, 2014). β-arrestin 2 knockout mice acutely treated with Δ^9-THC showed enhanced hypothermia and antinociception, as well as reduced tolerance development following chronic administration (Nguyen et al., 2012; Raehal and Bohn, 2014), but because traditional cannabinoid agonists function as unbiased ligands and cannot preferentially activate G protein-dependent signaling without recruiting β-arrestin 2, adverse effects such as dependence, tolerance and withdrawal will always be expected to occur following chronic exposure to traditional CB_1R agonists. Development of G-protein biased CB_1R agonists might minimize or avoid these adverse effects, thus improving the therapeutic profile of cannabinoid-based medications.

We have recently reported a novel class of indole quinuclidinone (IQD) analogues that represent a wholly new structural family of cannabinoid ligands, perhaps implying novel drug-receptor interactions (Ford et al., 2017). Unlike traditional CB_1R ligands, our lead compound PNR-4-20 functioned as a high efficacy agonist for modulation of G-protein dependent signaling via CB_1Rs in Chinese hamster ovary (CHO) cells, while recruiting little β-arrestin 2 and producing significantly less receptor desensitization and downregulation following chronic exposure. The G-protein biased agonism exhibited by PNR-4-20 at CB_1R thus represents a novel mechanism in cannabinoid pharmacology. *In vivo* studies confirmed that PNR-4-20 elicited dose-dependent CB_1R-mediated effects in the cannabinoid tetrad in the mouse, but consistent with the G-protein bias demonstrated *in vitro*, mice treated with PNR-4-20 once per day for 5 consecutive days exhibited reduced tolerance to hypothermic effects upon drug re-administration after a 7-day abstinence period, as compared to animals treated identically with either Δ^9-THC or JWH-018 (Ford et al., 2017). In those studies, in vivo effects were assessed at only a single timepoint after each drug administration, perhaps obscuring important differences among drugs. Similarly, assessment of rectal temperature might have been confounded by stress effects, which may have

been differentially modulated by the three cannabinoids tested. Nevertheless, additional studies also demonstrated dramatically reduced signs of rimonabant-precipitated withdrawal in mice chronically-treated with PNR-4-20, as compared to mice chronically treated with JWH-018 (Ford et al., 2017). Because FDA-approved cannabinoids like dronabinol and nabilone are utilized for chronic conditions like persistent nausea and wasting syndromes associated with cancer and AIDS (Guzman, 2003), we were here interested in further determining if chronic administration of PNR-4-20 would produce either reduced or less persistent tolerance to cannabinoid-induced effects when compared to unbiased CB_1R agonists. Using implantable radiotelemetry probes, we sought to non-invasively assess drug-elicited changes in core temperature over time in the much less stressful environment of the home cage. For the first time, we also assessed cross-tolerance to hypothermic effects between PNR-4-20 and Δ^9-THC, characterized tolerance to antinociceptive and cataleptic effects of PNR-4-20, JWH-018 and Δ^9-THC, and investigated CB_1R expression in therapeutically-relevant brain areas drawn from mice chronically administered PNR-4-20 or Δ^9-THC. Understanding the effects of chronic PNR-4-20 on different physiological endpoints in mice could further aid in the development of improved therapeutics based on this novel molecular scaffold.

6.0 Methods

Drugs

The indole quinuclidinone (IQD) analogue PNR-4-20 was synthesized in our laboratories, as previously described (Franks et al., 2014). WIN-55,212-2, and CP-55,940 were purchased from Tocris Bioscience (Bristol, United Kingdom). JWH-018 and Δ^9-THC were obtained from the NIDA Drug Supply Program (Bethesda, MD). Rimonabant was synthesized in the laboratory of Thomas E. Prisinzano, Ph.D., at the University of Kentucky School of Pharmacy, Department of Medicinal Chemistry (Lexington, KY). [^{3}H]CP-55,940 (175 Ci/mmol) was obtained from PerkinElmer (Waltham, MA). All other reagents used were purchased from Thermofisher

Scientific (Pittsburgh, PA). For *in vitro* assays, all cannabinoids were dissolved in 100% DMSO to 10 mM stock concentrations. For *in vivo* assays, all cannabinoids were dissolved in a vehicle containing ethanol, Tween 80 and saline at a ratio of 1:1:18. All injections were administered intraperitoneally (IP) at a constant volume of 0.01 cc/g.

Animals

All studies utilized adult male NIH-Swiss mice and were conducted in accordance with the Guide for Care and Use of Laboratory Animals as adopted and proclaimed by the National Institutes of Health. The University of Arkansas for Medical Sciences Institutional Animal Care and Use Committee approved all animal use protocols. All efforts were taken to minimize animal suffering and reduce the number of animals used. Mice were obtained from Harlan Laboratories, Inc. (Indianapolis, Indiana), arriving at 9 weeks of age and weighing between 20-25g. All subjects were housed three animals per cage (15.24 × 25.40 × 12.70 cm^3) in a temperature-controlled room in an Association for Assessment and Accreditation of Laboratory Animal Care–accredited animal facility. Room conditions were maintained at 22 ± 2°C and 45%–50% humidity, with lights set to a 12-hour light/dark cycle. Animals were fed Lab Diet rodent chow (Laboratory Rodent Diet no. 5001, PMI Feeds, St Louis, MO) *ad libitum* until immediately before testing.

Drug Administration

All test conditions used groups of either five or six mice, which were randomly assigned to experimental groups, and all mice were drug-naïve prior to the present studies. Based on our previous work (Ford et al., 2017), we studied doses of Δ^9-THC (30 mg/kg), JW-018 (3 mg/kg), and PNR-4-20 (100 mg/kg) producing comparable hypothermic effects in all of the *in vivo* assays below.

Biotelemetry of Core Temperature

Surgical preparation and real-time data collection using biotelemetry probes were conducted as previously described (Gannon et al., 2016). Briefly, the abdominal area of each mouse was shaved and sterilized with iodine swabs following anesthetization with inhaled isoflurane. A rostral-caudal cut approximately 1.5 cm in length was made with sterile skin scissors, providing access to the intraperitoneal cavity. A cylindrical glass-encapsulated radiotelemetry probe (model ER-4000 E-Mitter; Mini Mitter Co., Inc., Bend, OR) was then inserted, and the incision was closed using 5-0 absorbable suture material. Surgeries were carried out 14 days before initiation of each experiment, allowing time for incisions to heal. After surgery, all implanted mice were individually housed in 15.24 cm × 25.40 cm × 12.70 cm cages for the duration of all telemetry experiments. Implanted transmitters produced temperature-modulated signals that were sent to a receiver (model ER-4000 Receiver; Mini Mitter Co., Inc.) underneath each cage. Every 5 minutes, the computer collected data updates from the probes for core temperature readings (in degrees Celsius). After approximately 60 minutes of baseline data collection, mice were injected with either vehicle or test compound and returned to the telemetry stage for 24 hours of data collection. For rimonabant antagonism assays, 10 mg/kg rimonabant was administered 15 min prior to cannabinoid exposure. After rimonabant injection, mice were placed back into their home cages during this 15-min period.

Warm Water Tail Withdrawal

To measure tail withdrawal latency, each mouse was securely immobilized in the investigator's hand while the tail was allowed to hang freely. The distal 5 cm portion of the tail was dipped into a StableTemp (Cole-Parmer, Vernon Hills, IL) heat-controlled water bath maintained at 50°C, and a maximal latency cutoff time of 15 seconds was used to minimize tissue damage. Mice could remove their tails from the water at any point and the amount of time the tails remained in the water was measured with a stopwatch. Baseline tail withdrawal latencies ranged from 3 to 5 seconds. To ensure that tail withdrawal was due specifically to the nociceptive stimulus of the

JPET Fast Forward. Published on March 4, 2019 as DOI: 10.1124/jpet.118.252965
This article has not been copyedited and formatted. The final version may differ from this version.

50°C water and not a learned response over the course of multiple dips, a non-nociceptive control test with 45°C water was performed for each animal midway through the experimental session. On experimental test days, mice were injected with vehicle, 3 mg/kg JW-018, 30 mg/kg Δ^9-THC, or 100 mg/kg PNR-4-20. As previously determined, different pretreatment times were used for each drug in order to ensure maximal antinociceptive effects at the time of testing, such that 3 mg/kg JW-018 was administered 60 min prior to testing, 30 mg/kg Δ^9-THC was administered 45 min before testing, and PNR-4-20 was administered 35 min prior to testing. Because mice were injected every 24 hours for 5 days, a group of vehicle control mice were also tested to ensure that the effects observed across successive drug groups were due to drug-induced tolerance and not to confounding factors such as stress or hyperalgesia. To reduce stress-induced effects on analgesia, mice were acclimated to the procedure 1 week before drugs were administered. The habituation procedure was performed as previously described, except injections were excluded.

Catalepsy

Catalepsy was measured using the horizontal bar test, which employed a cylindrical steel bar (0.5 cm in diameter) that was supported 4.0 cm above a covered platform. The mice studied in warm water tail withdrawal assay were also used in this assay without any additional drug dosing. To begin each trial, mice were placed into a species-atypical position with hindlimbs on the platform and forelimbs on the horizontal bar. Upon placement on the catalepsy bar, a timer was started and counted until the mouse removed both paws from the bar. The maximum time allowed on the bar was 20 sec. Because we often observed habituation to the catalepsy procedure with repeated testing, animals were only tested for catalepsy on days 1, 5 and 12.

Cross-Tolerance Between PNR-4-20 and Δ^9-THC

Experiments investigating cross-tolerance to hypothermic effects were conducted as previously described (Tai et al., 2015). Briefly, two treatment groups of animals had biotelemetry

probes surgically implanted as described in *Methods 2.4.* Drug treatments for one group involved administration of 100 mg/kg PNR-4-20 every 24 hours for 4 days followed by an injection of 30 mg/kg Δ^9-THC on test day 5, while the other group received injections of 30 mg/kg Δ^9-THC every 24 hours for 4 days followed by an injection of 100 mg/kg PNR-4-20 on test day 5.

Tissue Collection and Membrane Preparation

Three separate groups of mice were administered vehicle, 30 mg/kg Δ^9-THC, or 100 mg/kg PNR-4-20 every 24 hours for 5 days. Twenty-four hours following the last injection, mice were euthanized via cervical dislocation and decapitation. Whole brains were immediately removed and hypothalamus and thalamus regions were hand dissected out on ice, then snap-frozen in liquid nitrogen and stored at −80°C. To prepare regional homogenates, dissected hypothalamus and thalamus were homogenized separately with 10 complete strokes utilizing a 40 mL Dounce glass homogenizer in ice-cold buffer containing 50 mM HEPES (pH 7.4), 3 mM $MgCl_2$, and 1 mM EDTA. Homogenized samples were then centrifuged at 40,000 × *g* for 10 min at 4°C. Supernatants were removed and pellets were re-suspended in ice-cold buffer, homogenized again, and centrifuged similarly two additional times. After the last centrifugation step, supernatants were removed and the remaining hypothalamus and thalamus membranes were re-suspended in ice-cold 50 mM HEPES, pH 7.4 to achieve an approximate protein concentration of 2 mg/ml. Membrane homogenates were divided into respective aliquots and stored at −80°C for future use. A 100 µl aliquot of each membrane preparation was removed prior to freezing and the protein concentration was determined using a BCA Protein Assay (Thermo Fisher Scientific, Waltham, MA).

Homologous Receptor Binding

Homologous receptor binding was performed as previously described (Brents et al., 2012). Briefly, respective reaction mixtures contained increasing concentrations of the non-radioactive

competing ligand CP55,940 in a 50 mM Tris-HCl buffer (pH 7.4) with 0.1% bovine serum albumin, 5 mM $MgCl_2$, 0.5 nM [^{3}H]-CP55,940, and either 20 µg of saline or drug treated hypothalamus membrane homogenates or 50 µg of treated vehicle or drug treated thalamus membrane homogenates. The total volume of the incubation mixture was 1 ml. All reactions were mixed and allowed to reach equilibrium binding via incubation at 37°C for 15 min. Non-specific binding was defined as the amount of radioligand binding remaining in the presence of a 1 µM concentration of the non-radioactive, high affinity, non-selective CBR agonist WIN-55,212-2. Binding was terminated via rapid vacuum filtration through glass fiber filters (Brandel, Gaithersburg, MD), followed by four 5 ml washes of ice-cold 50 mM Tris-HCl (pH 7.4) buffer containing 0.1% bovine serum albumin. Four ml of scintiverse scintillation fluid (Fisher Scientific, Waltham, MA) was added to respective filters and radioactivity was quantified 24 hr later utilizing liquid scintillation spectrophotometry

Statistical analyses

All data are presented as group means ± SEM (standard error of the mean). Points without error bars indicate that the variance is contained within the data point. For tolerance and cross tolerance studies, one-way repeated measures ANOVAs with Tukey's HSD *post-hoc* test compared the mean lowest temperature achieved after each injection (vehicle or each of 5 daily drug administration), as well as the lowest average temperature achieved in each drug group (represented as E_{MAX}). Area under the curve (AUC) between the average baseline temperature of vehicle treated animals and real-time core temperature readings of drug treated animals during a 300 min exposure window were calculated by subtracting the AUC beneath respective core temperature regressions from the AUC of the average baseline temperature. In the tables, E_{MAX} represents the lowest temperature achieved during each drug exposure while t_{MAX} shows the time (min) at which the lowest temperature occurred. These parameters were compared by one-way repeated measures ANOVA, followed by Dunnet's *post-hoc* test to compare all drug conditions to

the vehicle controls. For analgesia and catalepsy tests, a two-way repeated measures ANOVA, with day and drug as independent factors, followed by Tukey's HSD *post-hoc* test assessed differences amongst groups. Each *in vitro* data point presented in all figures is represented as the mean ± SEM from a minimum of 4 individual experiments. Three-parameter nonlinear regression for one-site homologous binding was used to determine the affinity (K_d) of [^{3}H]CP-55,940 and CB_1 receptor density (B_{MAX}) expression in crude whole mouse brain homogenates. One-way ANOVA's with Tukey's HSD *post-hoc* test was used to compare K_d and B_{MAX} values for respective compounds in thalamus and hypothalamus brain regions. All *in vivo* and *ex vivo* statistical calculations were performed using GraphPad Prism version 7.03 (GraphPad Software Inc., Le Jolla, CA), and statistical significance was always judged at $P<0.05$.

7.0 Results

Mice chronically treated with 100 mg/kg PNR-4-20 exhibited less tolerance to cannabinoid induced hypothermic effects when compared to 30 mg/kg Δ^9-THC.

Core temperatures following administration of vehicle, 30 mg/kg Δ^9-THC (Fig 1A) or 100 mg/kg PNR-4-20 (Fig 1D) were significantly different among groups ($F(2,14)=47.88$ for Δ^9-THC; $F(2,12)=13.06$ for PNR-4-20; $P<0.05$ for both comparisons.) Indeed, both Δ^9-THC ($q=12.01$, $P<0.05$) and PNR-4-20 ($q=6.233$, $P<0.05$) elicited hypothermic effects which were significantly different from those observed following vehicle administration. Importantly, the hypothermic effects of both Δ^9-THC and PNR-4-20 were completely blocked by prior administration of 10 mg/kg of the selective CB_1R antagonist/inverse agonist, rimonabant. Statistical testing revealed that core temperatures following rimonabant + Δ^9-THC ($q=0.787$, $P>0.05$) or rimonabant + PNR-4-20 ($q=0.052$, $P>0.05$) did not differ from those observed following vehicle injection. Importantly, the AUC for hypothermic effects (calculated for each individual animal making up the mean data presented in Figures 1B and 1E) were not significantly different for Δ^9-THC and PNR-4-20 when either drug was administered to naïve mice ($q=2.078$, $P>0.05$).

JPET Fast Forward. Published on March 4, 2019 as DOI: 10.1124/jpet.118.252965
This article has not been copyedited and formatted. The final version may differ from this version.

When mice were injected with either Δ^9-THC or PNR-4-20 for 5 consecutive days, changes in E_{MAX}, t_{MAX} and area under the curve (AUC) were apparent across days (Table 1). Δ^9-THC produced a significant drop in core body temperature ($F(6,24)=10.684$, $P<0.05$) as compared to vehicle administration, but this effect depended on the number of times the drug was administered (Fig 1C). Following the initial injection, core temperature dropped ~4°C, and as mice were repeatedly treated every 24 hours for the remaining 4 days, development of tolerance was apparent as indicated by a progressive blunting of Δ^9-THC-induced hypothermia. Indeed, only the first ($q=10.005$, $P<0.05$) and second ($q=5.879$m $P<0.05$) daily Δ^9-THC injections elicited hypothermic effects which were different from those observed following vehicle injection, while the third ($q=7.358$, $P<0.05$), fourth ($q=7.521$, $P<0.05$) and fifth ($q=7.843$, $P<0.05$) daily injections elicited effects which were significantly different from those observed after the first Δ^9-THC injection. No other between-day comparisons were significant during this 5-day period of repeated drug administration. When retested with Δ^9-THC after a 14-day drug abstinence period, persistent tolerance was noted, as the hypothermic effects observed were different from both vehicle treatment ($q=4.972$, $P<0.05$) and the initial Δ^9-THC injection ($q=5.033$, $P<0.05$) (Fig 1C; Table 1). Similarly, PNR-4-20 also produced a significant drop in core body temperature ($F(6,24)=10.364$, $P<0.05$) as compared to vehicle administration, but this effect also depended on the number of times the drug was administered (Fig 1F). Following the initial injection, core temperature dropped by ~3 °C, but as mice were repeatedly treated every 24 hours for the remaining 4 days, an unusual pattern of acute tolerance development emerged (Fig 1F). Like Δ^9-THC, the first ($q=8.623$, $P<0.05$) and second ($q=5.734$, $P<0.05$) PNR-4-20 injection elicited hypothermic effects which were different from those observed following vehicle injection, while the third ($q=6.855$, $P<0.05$) injection elicited effects which were significantly different from those observed after the first PNR-4-20 administration, but were not different from the vehicle control ($q=1.769$, $P>0.05$). Interestingly, the fourth and fifth PNR-4-20 injections again elicited hypothermic effects which were different from the vehicle control ($q=4.727$ for injection 4 and $q=4.945$ for injection 5, $P<0.05$

for both comparisons), but were also significantly different from the hypothermic effects observed following the initial administration of the drug (q=5.216 for injection 4 and q=4.624 for injection 5, P<0.05 for both comparisons. No other between-day comparisons were significant during this 5-day period of repeated drug administration. After the 14-day drug abstinence period, PNR-4-20 elicited hypothermic effects which were significantly different from the vehicle control (q=3.353, P<0.05), but not from the initial drug administration (q=0.270, P>0.05), with E_{MAX} and a t_{MAX} values also similar to those observed after the initial treatment (Fig 1F and Table 1). Thus, PNR-4-20 and Δ^9-THC both produced CB_1R-mediated hypothermia *in vivo*, but distinctions in both acute and persistent tolerance were observed between these drugs.

Mice chronically treated with 100 mg/kg PNR-4-20 exhibited less tolerance to cannabinoid-induced antinociception and catalepsy.

In antinociception studies (Fig 2A), significant effects of drug (F(3,100)=85.677) and of day (F(5,100)=52.120) were observed, and the interaction of these two factors was also significant (F(15,100)=4.573) (P<0.05 for all comparisons.) Following repeated vehicle injection (Fig 2A, open circles), no significant differences in tail withdrawal latencies were observed across days (P>0.05 for all comparisons.) For daily Δ^9-THC administrations (Fig 2A, filled circles), significant differences from the vehicle controls were observed on days 1 (q=12.572) and 2 (q=5.944), and the initial antinociceptive effect noted on day 1 was significantly different from that observed on days 2 (q=6.678), 3 (q=10.401), 4 (q=10.707) and 5 (q=10.973) (P<0.05 for all comparisons). The antinociceptive effect noted on day 2 was also different from that observed on day 5 (q=4.294, P<0.05), but no other between-day comparisons were significant during this 5-day period of repeated Δ^9-THC administration. For daily JWH-018 administrations (Fig 2A, filled triangles), significant differences from the vehicle controls were observed on days 1 (q=11.936), 2 (q=8.372), 3 (q=4.621) and 4 (q=4.145), and the initial antinociceptive effect noted on day 1 was significantly different from that observed on days 3 (q=7.433), 4 (q=8.867) and 5 (q=10.847) (P<0.05 for all

JPET Fast Forward. Published on March 4, 2019 as DOI: 10.1124/jpet.118.252965
This article has not been copyedited and formatted. The final version may differ from this version.

comparisons). The antinociceptive effect noted on day 2 was also different from that observed on days 4 (q=5.282) and 5 (q=7.262) (P<0.05 for both comparisons), but no other between-day comparisons were significant during this 5-day period of repeated JWH-018 administration. For daily PNR-4-20 administrations (Fig 2A, open diamonds), significant differences from the vehicle controls were observed on days 1 (q=9.427), 2 (q=6.741) and 4 (q=5.875), and the initial antinociceptive effect noted on day 1 was significantly different from that observed on days 3 (q=6.558), 4 (q=4.588) and 5 (q=6.697) (P<0.05 for all comparisons). No other between-day comparisons were significant during this 5-day period of repeated PNR-4-20 administration. Interestingly, when animals were retested after a seven-day drug abstinence period, residual tolerance was apparent for animals treated with JWH-018 and Δ^9-THC (Fig 2B), but not in mice treated with PNR-4-20. Tail withdrawal latencies significantly less than those observed following the first drug administration were quantified after the abstinence period for Δ^9-THC (q=11.697) and for JWH-018 (q=8.210) (P<0.05 for both comparisons), but not for PNR-4-20 (q=2.399, P>0.05).

To study the cataleptic effects of JWH-018, Δ^9-THC, and PNR-4-20 across repeated treatments, mice were injected as described above. Because habituation to the testing procedure over repeated days confounds the results, mice were only tested on the horizontal bar on days 1 and 5, and then again after the 7-day abstinence period on day 12. Animals repeatedly treated with JWH-018 showed pronounced tolerance to cataleptic effects on day 5 (t=5.772, P<0.05), and this tolerance was still apparent during the retest on day 12 (t=5.433, P<0.05) (Fig 3). Similarly, repeated testing with Δ^9-THC resulted in reduced catalepsy scores on days 5 and 12, although large intersubject variability in the initial catalepsy scores observed on day 1 precluded statistical significance. In contrast, PNR-4-20 elicited cataleptic effects at a similar level across the three tests, and no apparent tolerance was observed on days 5 or 12.

Cross-tolerance to hypothermic effects among PNR-4-20 and Δ^9-THC

JPET Fast Forward. Published on March 4, 2019 as DOI: 10.1124/jpet.118.252965
This article has not been copyedited and formatted. The final version may differ from this version.

Because PNR-4-20 elicits a distinct tolerance profile across repeated administration in mice, the potential for cross-tolerance to cannabinoid-induced hypothermia between PNR-4-20 and Δ^9-THC was investigated. Fig 4A presents time-activity data for core temperature following injection of PNR-4-20 for days 1 and 4 with Δ^9-THC being administered on day 5. Statistical analysis of the lowest core temperature observed across all treatment days (Fig 4B) detected hypothermic effects of all PNR-4-20 administrations when compared to the vehicle control ($q=13.779$, 7.504, 6.288 and 5.752 for injections 1-4, respectively, $P<0.05$ for all comparisons) and for the Δ^9-THC cross-tolerance test on day 5 ($q=8.975$, $P<0.05$). However, hypothermic effects elicited by the initial injection of PNR-4-20 significantly differed from those of all subsequent drug administrations ($q=6.275$ for injection 2, $q=7.491$ for injection 3, $q=8.027$ for injection 4, and $q=4.804$ for the Δ^9-THC cross-tolerance test on day 5) ($P<0.05$ for all comparisons). Importantly, challenge with Δ^9-THC on day 5 revealed apparent hypothermic effects with maximal temperature reductions similar to those observed following the final dose of PNR-4-20, but with a much longer duration of action (see Table 2), similar to that typically observed with an initial administration of Δ^9-THC to drug-naïve mice.

Similarly, Fig 4C presents time-activity data for core temperature following injection of Δ^9-THC for days 1 and 4 with PNR-4-20 being administered on day 5. Statistical analysis of the lowest core temperature observed across all treatment days (Fig 4D) detected hypothermic effects of the first two injections of Δ^9-THC when compared to the vehicle control ($q=9.399$ and 5.399, respectively, $P<0.05$ for both comparisons), but not for days 3 or 4 ($q=4.022$ and 3.045, respectively, $P>0.05$ for both comparisons.) During the cross-tolerance test with PNR-4-20 on day 5, no significant hypothermic effects were observed ($q=3.124$, $P>0.05$). However, hypothermic effects elicited by the initial injection of Δ^9-THC significantly differed from those of the third and fourth drug administrations ($q=5.377$ and 6.354, respectively, $P<0.05$ for both comparisons), as did the hypothermic effects induced by the PNR-4-20 cross-tolerance test on day 5 ($q=6.275$, $P<0.05$). Importantly, administration of PNR-4-20 on the last day induced

JPET Fast Forward. Published on March 4, 2019 as DOI: 10.1124/jpet.118.252965
This article has not been copyedited and formatted. The final version may differ from this version.

hypothermic effects which were not significantly different from those produced by the 4th Δ^9-THC injection, despite the higher *in vitro* efficacy of PNR-4-20 at CB_1Rs (see Table 2). Collectively, these data suggest an asymmetrical cross-tolerance among Δ^9-THC and PNR-4-20, as animals administered PNR-4-20 for 4 days showed significant hypothermia when challenged with Δ^9-THC, while animals repeatedly administered Δ^9-THC and challenged with PNR-4-20 did not.

Repeated treatment with PNR-4-20 produces less CB_1R downregulation in the hypothalamus and thalamus than the unbiased agonist Δ^9-THC.

Prolonged treatment with Δ^9-THC in naïve mice resulted in 64% and 74% reductions in CB_1R expression (*e.g.,* B_{MAX} values) in the hypothalamus (Fig 5A) and thalamus (Fig 5B), respectively, relative to vehicle treated animals ($q=10.200$ and 5.812, respectively, $P<0.05$ for both comparisons). Repeated PNR-4-20 treatment also significantly reduced CB_1R levels relative to vehicle in the hypothalamus (Fig 5A, $q=4.549$, $P<0.05$), but the degree of down-regulation was significantly less than that produced by Δ^9-THC ($q=5.655$, $P<0.05$). Interestingly, in the thalamus, chronic PNR-4-20 treatment did not significantly reduce CB_1R density ($q=1.359$, $P>0.05$). Despite the in alterations in B_{MAX}, no treatment produced a significant alteration in the affinity (*e.g.,* K_d values) of CP-55,940 in either brain region studied.

8.0 Discussion

Drugs which selectively signal through G protein dependent pathways can elicit therapeutic effects with reduced adverse effects. As seen with the G protein biased μ-opioid agonist oliceridine (formerly TRV130), antinociception can be induced with minimal adverse effects associated with acute (i.e., gastrointestinal inhibition and respiratory depression) or chronic (i.e., analgesic tolerance) administration (Soergel et al., 2014). Additionally, the G protein biased κ-opioid agonist triazole 1.1 produced antinociceptive and anti-pruritic effects without inducing significant sedation or dysphoria (Brust et al., 2016). We believe IQD-derived PNR-4-20

JPET Fast Forward. Published on March 4, 2019 as DOI: 10.1124/jpet.118.252965
This article has not been copyedited and formatted. The final version may differ from this version.

is the first G protein biased cannabinoid agonist developed, but despite the precedent set by the biased opioid agonists, the data here presented for PNR-4-20 only partially follows this pattern of preserved therapeutic effects with reduced adverse effects.

In this regard, acute antinociceptive effects of PNR-4-20 were obtained in the warm water tail withdrawal assay, and these effects were similar in magnitude to those of the unbiased cannabinoid agonists Δ^9-THC and JWH-018, suggesting that the reduced recruitment of β-arrestins by PNR-4-20 may not impair its therapeutic utility in the realm of pain management. However, antinociceptive tolerance was clearly observed with chronic administration of PNR-4-20, and this progressive reduction in effect occurred at a similar rate and to a similar extent as seen with unbiased Δ^9-THC and JWH-018. However, it is important to note that imposition of a drug abstinence period no longer than 7 days was sufficient to completely restore antinociceptive efficacy of PNR-4-20, and this was dramatically different than the persistent tolerance to antinociceptive effects observed with the same chronic regimens of comparably-effective doses of Δ^9-THC and JWH-018. A similar distinction can be drawn between the cataleptic effects of PNR-4-20, Δ^9-THC and JWH-018, as no apparent tolerance was observed with PNR-4-20 on this endpoint while complete and persistent tolerance was observed with the two unbiased cannabinoid agonists. Although cannabinoid-elicited catalepsy is not a particularly useful therapeutic effect, the complete lack of tolerance development here observed with PNR-4-20 lends proof-of-concept to the notion that G protein biased agonists may be capable of circumventing the standard progressive reduction in effect observed with chronic administration of unbiased cannabinoid agonists. Future drug design efforts with the IQD scaffold may identify novel compounds which resist tolerance to more therapeutically-relevant endpoints, like antinociceptive effects.

While it is possible that a shorter duration of hypothermic action for PNR-4-20 relative to THC might constitute a potential mechanism to explain the reduced tolerance here presented, we believe that this is unlikely for two reasons. First, we have previously reported that similar to PNR-

4-20 reported here, JWH-018 also exhibits a shorter duration of action in the cannabinoid tetrad relative to THC (Brents et al., 2011), but elicits similar tolerance development to hypothermic effects as that observed with THC (Tai et al., 2015). Nevertheless, the duration of PNR-4-20-elicited hypotherkic effects is shorter than that of JWH-018, and the maximal hypothermic effects of PNR-4-20 (at doses straining the limit of solubility) are smaller in magnitude than those of JWH-018. n agreement with those previous studies, and in spite of differences in their durations of action, we report in the present study (Figure 2) that both JWH-018 and THC produce greater levels of tolerance relative to PNR-4-20. Second, the AUC for hypothermic effects elicited by THC (Figure 1B) and PNR-4-20 (Figure 1E) on day 1 of treatment were not significantly different from one another. Although additional pharmacokinetic studies of PNR-4-20 could potentially add mechanistic insight, the data presented here were primarily designed only as an initial study to compare the *in vitro* versus *in vivo* effects of the first G-protein biased CB_1R agonist to unbiased CB_1R agonists. Importantly, the purpose of these designed studies was met by the data presented (*e.g.,* demonstrating differences between biased and unbiased CB_1R agonists). We nevertheless believe that comprehensive pharmacokinetic studies should be conducted with PNR-4-20 and other novel compounds exhibiting G-protein bias at CB_1Rs as part of future drug development efforts.

Studies investigating cross-tolerance between PNR-4-20 and Δ^9-THC further revealed novel *in vivo* functionality of our lead compound. Data from these studies suggest that the hypothermic effects of both PNR-4-20 and Δ^9-THC diminished over repeated administration, but while complete and persistent tolerance to hypothermic effects of Δ^9-THC were apparent, significant hypothermic effects of PNR-4-20 re-emerged with continued treatment, and no evidence of residual tolerance was observed when animals were tested again after a 14-day drug abstinence. This represents a dramatic difference between the effects of chronic Δ^9-THC and PNR-4-20, which is further reflected in the non-reciprocal cross-tolerance observed between these two drugs. Specifically, administration of Δ^9-THC to mice previously treated with PNR-4-20

for 4 consecutive days resulted in significant hypothermic effects which were comparable (in terms of duration) to those observed following administration of Δ^9-THC to drug-naïve mice. On the other hand, administration of PNR-4-20 to mice previously treated with Δ^9-THC resulted in an attenuated hypothermic effect which was not statistically distinguishable from injection of the drug vehicle. This later finding is not necessarily surprising, as the aminoalkylindole full CB_1R agonists JWH-018 and JWH-073 both also failed to surmount tolerance to hypothermic effects (measured as core temperature with radiotelemetry) elicited by Δ^9-THC in NIH Swiss mice treated identically to those in the present studies (Tai et al., 2015), but tolerance to hypothermic effects elicited by a different chronic regimen of Δ^9-THC (measured as rectal temperature by insertion of a thermoprobe) were partially surmounted by administration of structurally distinct CB_1R high efficacy agonists WIN 55,212 and CP 55,940 in ICR mice (Fan et al., 1994). Because cannabinoid agonists typically desensitize and downregulate CB_1Rs through recruitment of β-arrestins, it is expected that treatment with any unbiased agonist would likely decrease the effects of subsequent treatment with a different agonist. But the pattern of data obtained here suggests that the effects of repeated exposure to PNR-4-20 results in different regulatory effects on CB_1Rs than what is typically observed with unbiased agonists like Δ^9-THC. This is supported by our present data demonstrating that chronic PNR-4-20, at the doses here tested, elicits absolutely no downregulation of CB_1Rs in the thalamus, and dramatically attenuated downregulation of CB_1Rs (as compared to Δ^9-THC) in the hypothalamus.

The CB_1/CB_2R agonist [^{3}H]CP55,940 was used to quantify CB_1R downregulation in this study. As an agonist, this radioligand can exhibit biphasic binding kinetics, binding to both high and low affinity states of the receptor. It is possible that repeated drug treatment in the present study may reduce the pool of G-proteins available for receptor coupling, and/or affect coupling of G-proteins to the receptor. If so, this might be reflected as an apparent decrease in receptor binding, even though it would actually represent only a decrease in proportion of receptors in high

affinity state and not in total receptor number. It can therefore not conclusively be stated that reductions in B_{MAX} observed are due solely to receptor downregulation, as changes in receptor/G-protein stoichiometry and receptor desensitization could affect high affinity binding, and appear as a decrease in B_{MAX}. The question could be conclusively answered by future studies using antagonist radioligands to quantify receptor density, which typically exhibit similar affinity for both low and high affinity sites.

We have previously demonstrated that the G protein vs. β-arrestin 2 bias factor for PNR-4-20 was 29.5, which compares quite favorably with the G protein bias factors reported for other drugs, such as the bias factor of ~3 reported for oliceridine. Nevertheless, the initial tolerance development to antinociceptive and hypothermic effects of PNR-4-20 is perhaps explainable by the *in vitro* observations that repeated treatment with PNR-4-20 did result in rapid recruitment of β-arrestin 2, producing desensitization and downregulation of CB_1Rs (Ford et al., 2017). Importantly, PNR-4-20 treated cells, but not CP 55,940 treated cells, recovered from agonist induced desensitization and downregulation at later timepoints. While comprehensive studies investigating downstream signaling cascades have yet to be conducted with PNR-4-20 at CB_1Rs, these studies would likely provide mechanistic explanations for the lack of persistent tolerance to PNR-4-20 effects such as those presently demonstrated in mice, and may also explain the apparent reversal of tolerance to hypothermic effects here demonstrated.

We have previously demonstrated orderly dose-effect relationships for PNR-4-20 in the cannabinoid tetrad in mice, and shown that these effects are blocked by prior administration of the CB_1R inverse agonist / antagonist rimonabant (Ford et al., 2017). Nevertheless, the relatively poor solubility of PNR-4-20 probably prevents us from capturing the true maximal effects of this drug *in vivo*, as we routinely observe larger hypothermic effects with aminalkylindole-derived synthetic cannabinoid agonists with similar efficacy (in terms of G protein signaling) as PNR-4-20 (i.e., Tai et al., 2015). To address this issue, other CB_1R G protein biased IQD analogues such

as PNR-4-02 (Ford et al., 2017) should be considered for further *in vivo* analysis. Characterizing the *in vivo* profile of multiple IQD analogues could potentially aid in the development of G protein biased compounds that have improved drug-like properties. Additionally, studies investigating downregulation and desensitization of CB_1Rs in mice repeatedly treated with PNR-4-20 also need to be expanded upon. Specifically, only homologous receptor binding was performed on hypothalamus and thalamus brain regions. While measurements of receptor density are important in determining changes CB_1R expression, functional assays measuring G protein function and downstream effector modulation should be conducted in future experiments to determine if receptor desensitization occurs following repeated dosing of PNR-4-20. While CB_1Rs in the hypothalamus and thalamus mediate temperature regulation as well as pain perception (Cross, 1994; Martin et al., 1996; Fonseca et al., 2014), other brain regions associated with nociception and catalepsy (*e.g.*, spinal cord, periaqueductal gray, caudate-putamen, and globus pallidus) should be investigated as well.

Alongside exploratory mechanistic studies of PNR-4-20, additional *in vivo* studies investigating the potential abuse liability of the IQD drug class using drug discrimination and self-administration assays should be conducted. Because PNR-4-20 exhibits a distinct pharmacological profile at CB_1Rs, most likely related to its G protein biased agonism, substituting PNR-4-20 in a drug discrimination assay where subjects have been trained to discriminate Δ^9-THC from saline would potentially reveal whether the interoceptive effects of this novel compound are similar to or distinct from those of traditional unbiased cannabinoids. As previously established with JWH-018 and JWH-073 in mice that were trained to discriminate Δ^9-THC from saline, cannabinoid agonists with differing intrinsic CB_1R efficacies nonetheless cross-substitute for one another in drug discrimination assays (Wiley et al., 2014). Whether this also applies to CB_1R agonists with different signaling profiles remains to be determined. Furthermore, self-administration assays would allow one to determine if PNR-4-20 produced reinforcing effects which are typically predictive of abuse liability in humans. Some studies have shown that high

efficacy agonists like JWH-018, but not low efficacy agonists like Δ^9-THC, produce positive reinforcing effects in animal subjects (De Luca et al., 2015). Whether a biased CB_1R agonist like PNR-4-20 would exhibit reduced reinforcing effects should be investigated. Understanding the effects of PNR-4-20 on operant behavior, including assays like drug discrimination and self-administration could reveal how ligands with novel molecular signaling properties may induce unique behavioral effects.

Overall, the present studies suggest that the IQD analogue PNR-4-20 elicits unique effects when administered repeatedly to NIH Swiss mice. These effects clearly differentiate PNR-4-20 from traditional, unbiased cannabinoid agonists such as Δ^9-THC and JWH-018. Importantly, results from these studies reveal that PNR-4-20 elicits significantly less tolerance to hypothermic and cataleptic effects, as well as less persistent antinociceptive tolerance following chronic administration, than non-biased CB1 agonists. This is consistent with its proposed biased signaling through G proteins relative to β-arrestins. Future drug development efforts with the IQD scaffold may identify additional cannabinoids biased toward beneficial G protein signaling over β-arrestin 2 recruitment, perhaps resulting in novel therapeutics for difficult disease states.

9.0 Acknowledgements

We thank the UAMS Division of Laboratory Animal Medicine for expert husbandry services and Thomas Prisinzano, Ph.D. in the Department of Medicinal Chemistry at the University of Kansas School of Pharmacy (Lawrence, KS) for providing rimonabant as a generous gift.

10.0 Author Contributions

Participated in research design: Ford, Cabanlong, Tai, Franks, Fantegrossi, Prather

Conducted experiments: Ford, Cabanlong, Tai, Franks, Fantegrossi

Contributed new reagents or analytic tools: Penthala, Crooks

Performed data analysis: Ford, Fantegrossi, Prather

Wrote or contributed to the writing of the manuscript: Ford, Fantegrossi, Prather

11.0 References

Berlach DM, Shir Y and Ware MA (2006) Experience with the synthetic cannabinoid nabilone in chronic noncancer pain. *Pain Med* **7**:25-29.

Birnbaumer L, Codina J, Mattera R, Cerione RA, Hildebrandt JD, Sunyer T, Rojas FJ, Caron MG, Lefkowitz RJ and Iyengar R (1985) Regulation of hormone receptors and adenylyl cyclases by guanine nucleotide binding N proteins. *Recent Prog Horm Res* **41**:41-99.

Brents LK, Gallus-Zawada A, Radominska-Pandya A, Vasiljevik T, Prisinzano TE, Fantegrossi WE, Moran JH and Prather PL (2012) Monohydroxylated metabolites of the K2 synthetic cannabinoid JWH-073 retain intermediate to high cannabinoid 1 receptor (CB1R) affinity and exhibit neutral antagonist to partial agonist activity. *Biochem Pharmacol* **83**:952-961.

Brents LK, Reichard EE, Zimmerman SM, Moran JH, Fantegrossi WE and Prather PL (2011) Phase I hydroxylated metabolites of the K2 synthetic cannabinoid JWH-018 retain in vitro and in vivo cannabinoid 1 receptor affinity and activity. *PLoS One* **6**:c21917.

Brust TF, Morgenweck J, Kim SA, Rose JH, Locke JL, Schmid CL, Zhou L, Stahl EL, Cameron MD, Scarry SM, Aube J, Jones SR, Martin TJ and Bohn LM (2016) Biased agonists of the kappa opioid receptor suppress pain and itch without causing sedation or dysphoria. *Sci Signal* **9**:ra117.

Casey PJ and Gilman AG (1988) G protein involvement in receptor-effector coupling. *J Biol Chem* **263**:2577-2580.

Cooper ZD, Comer SD and Haney M (2013) Comparison of the analgesic effects of dronabinol and smoked marijuana in daily marijuana smokers. *Neuropsychopharmacology* **38**:1984-1992.

Cressey D (2015) The cannabis experiment. *Nature* **524**:280-283.

Cross SA (1994) Pathophysiology of pain. *Mayo Clin Proc* **69**:375-383.

De Luca MA, Bimpisidis Z, Melis M, Marti M, Caboni P, Valentini V, Margiani G, Pintori N, Polis I, Marsicano G, Parsons LH and Di Chiara G (2015) Stimulation of in vivo dopamine transmission and intravenous self-administration in rats and mice by JWH-018, a Spice cannabinoid. *Neuropharmacol* **99**:705-714.

Devane WA, Dysarz FA, 3rd, Johnson MR, Melvin LS and Howlett AC (1988) Determination and characterization of a cannabinoid receptor in rat brain. *Mol Pharmacol* **34**:605-613.

Devinsky O, Cross JH, Laux L, Marsh E, Miller I, Nabbout R, Scheffer IE, Thiele EA, Wright S and Cannabidiol in Dravet Syndrome Study G (2017) Trial of Cannabidiol for Drug-Resistant Seizures in the Dravet Syndrome. *N Engl J Med* **376**:2011-2020.

Eisenstein M (2015) Medical marijuana: Showdown at the cannabis corral. *Nature* **525**:S15-17.

Fonseca CG, Pires W, Lima MR, Guimaraes JB, Lima NR and Wanner SP (2014) Hypothalamic temperature of rats subjected to treadmill running in a cold environment. *PLoS One* **9**:e111501.

Ford BM, Franks LN, Tai S, Fantegrossi WE, Stahl EL, Berquist MD, Cabanlong CV, Wilson CD, Penthala NR, Crooks PA and Prather PL (2017) Characterization of structurally novel G protein biased CB1 agonists: Implications for drug development. *Pharmacol Res* **125**:161-177.

Franks LN, Ford BM, Madadi NR, Penthala NR, Crooks PA and Prather PL (2014) Characterization of the intrinsic activity for a novel class of cannabinoid receptor ligands: Indole quinuclidine analogs. *Eur J Pharmacol* **737**:140-148.

Gannon BM, Williamson A, Suzuki M, Rice KC and Fantegrossi WE (2016) Stereoselective Effects of Abused "Bath Salt" Constituent 3,4-Methylenedioxypyrovalerone in Mice: Drug Discrimination, Locomotor Activity, and Thermoregulation. *J Pharmacol Exp Ther* **356**:615-623.

Guzman M (2003) Cannabinoids: potential anticancer agents. *Nat Rev Cancer* **3**:745-755.

Horswill JG, Bali U, Shaaban S, Keily JF, Jeevaratnam P, Babbs AJ, Reynet C and Wong Kai In P (2007) PSNCBAM-1, a novel allosteric antagonist at cannabinoid CB1 receptors with hypophagic effects in rats. *Br J Pharmacol* **152**:805-814.

Howlett AC, Barth F, Bonner TI, Cabral G, Casellas P, Devane WA, Felder CC, Herkenham M, Mackie K, Martin BR, Mechoulam R and Pertwee RG (2002) International Union of Pharmacology. XXVII. Classification of cannabinoid receptors. *Pharmacol Rev* **54**:161-202.

Law PY, Hom DS and Loh HH (1985) Multiple affinity states of opiate receptor in neuroblastoma x glioma NG108-15 hybrid cells. Opiate agonist association rate is a function of receptor occupancy. *J Biol Chem* **260**:3561-3569.

Lynch ME and Ware MA (2015) Cannabinoids for the Treatment of Chronic Non-Cancer Pain: An Updated Systematic Review of Randomized Controlled Trials. *J Neuroimmune Pharmacol* **10**:293-301.

Madadi NR, Penthala NR, Brents LK, Ford BM, Prather PL and Crooks PA (2013) Evaluation of (Z)-2-((1-benzyl-1H-indol-3-yl)methylene)-quinuclidin-3-one analogues as novel, high affinity ligands for CB1 and CB2 cannabinoid receptors. *Bioorg Med Chem Lett* **23**:2019-2021.

Maida V and Daeninck PJ (2016) A user's guide to cannabinoid therapies in oncology. *Curr Oncol* **23**:398-406.

Martin WJ, Hohmann AG and Walker JM (1996) Suppression of noxious stimulus-evoked activity in the ventral posterolateral nucleus of the thalamus by a cannabinoid agonist: correlation between electrophysiological and antinociceptive effects. *J Neurosci* **16**:6601-6611.

Matsuda LA, Lolait SJ, Brownstein MJ, Young AC and Bonner TI (1990) Structure of a cannabinoid receptor and functional expression of the cloned cDNA. *Nature* **346**:561-564.

Muramatsu RS, Silva N and Ahmed I (2013) Suspected dronabinol withdrawal in an elderly cannabis-naive medically ill patient. *Am J Psychiatry* **170**:804.

Nguyen PT, Schmid CL, Raehal KM, Selley DE, Bohn LM and Sim-Selley LJ (2012) beta-arrestin2 regulates cannabinoid CB1 receptor signaling and adaptation in a central nervous system region-dependent manner. *Biol Psychiatry* **71**:714-724.

Pergolizzi JV, Jr., Taylor R, LeQuang JA, Zampogna G and Raffa RB (2017) Concise review of the management of iatrogenic emesis using cannabinoids: emphasis on nabilone for chemotherapy-induced nausea and vomiting. *Cancer Chemother Pharmacol* **79**:467-477.

Pertwee RG (1997) Pharmacology of cannabinoid CB1 and CB2 receptors. *Pharmacol Ther* **74**:129-180.

Pertwee RG (2006) The pharmacology of cannabinoid receptors and their ligands: an overview. *Int J Obes (Lond)* **30 Suppl 1**:S13-18.

Piscitelli F, Ligresti A, La Regina G, Coluccia A, Morera L, Allara M, Novellino E, Di Marzo V and Silvestri R (2012) Indole-2-carboxamides as allosteric modulators of the cannabinoid CB(1) receptor. *J Med Chem* **55**:5627-5631.

Price MR, Baillie GL, Thomas A, Stevenson LA, Easson M, Goodwin R, McLean A, McIntosh L, Goodwin G, Walker G, Westwood P, Marrs J, Thomson F, Cowley P, Christopoulos A, Pertwee RG and Ross RA (2005) Allosteric modulation of the cannabinoid CB1 receptor. *Mol Pharmacol* **68**:1484-1495.

Raehal KM and Bohn LM (2014) beta-arrestins: regulatory role and therapeutic potential in opioid and cannabinoid receptor-mediated analgesia. *Handb Exp Pharmacol* **219**:427-443.

Reuter SE and Martin JH (2016) Pharmacokinetics of Cannabis in Cancer Cachexia-Anorexia Syndrome. *Clin Pharmacokinet* **55**:807-812.

Rosenberg EC, Patra PH and Whalley BJ (2017) Therapeutic effects of cannabinoids in animal models of seizures, epilepsy, epileptogenesis, and epilepsy-related neuroprotection. *Epilepsy Behav* **70**:319-327.

Soergel DG, Subach RA, Burnham N, Lark MW, James IE, Sadler BM, Skobieranda F, Violin JD and Webster LR (2014) Biased agonism of the mu-opioid receptor by TRV130 increases analgesia and reduces on-target adverse effects versus morphine: A randomized, double-blind, placebo-controlled, crossover study in healthy volunteers. *Pain* **155**:1829-1835.

Tai S, Hyatt WS, Gu C, Franks LN, Vasiljevik T, Brents LK, Prather PL and Fantegrossi WE (2015) Repeated administration of phytocannabinoid Delta(9)-THC or synthetic cannabinoids JWH-018 and JWH-073 induces tolerance to hypothermia but not locomotor suppression in mice, and reduces CB1 receptor expression and function in a brain region-specific manner. *Pharmacol Res* **102**:22-32.

Verty AN, Evetts MJ, Crouch GJ, McGregor IS, Stefanidis A and Oldfield BJ (2011) The cannabinoid receptor agonist THC attenuates weight loss in a rodent model of activity-based anorexia. *Neuropsychopharmacology* **36**:1349-1358.

Vickroy TW, Watson M, Yamamura HI and Roeske WR (1984) Agonist binding to multiple muscarinic receptors. *Fed Proc* **43**:2785-2790.

Volkow ND, Baler RD, Compton WM and Weiss SR (2014) Adverse health effects of marijuana use. *N Engl J Med* **370**:2219-2227.

Ware MA, Daeninck P and Maida V (2008) A review of nabilone in the treatment of chemotherapy-induced nausea and vomiting. *Ther Clin Risk Manag* **4**:99-107.

Weinstein AM and Gorelick DA (2011) Pharmacological treatment of cannabis dependence. *Curr Pharm Des* **17**:1351-1358.

Wiley JL, Lefever TW, Cortes RA and Marusich JA (2014) Cross-substitution of Delta9-tetrahydrocannabinol and JWH-018 in drug discrimination in rats. *Pharmacol Biochem Behav* **124**:123-128.

12.0 Footnotes

This work was supported, in part, by the National Institutes of Health National Institute on Drug Abuse [Grants DA039143 and DA022981], by the National Institute on General Medical Sciences [IDeA Program award GM110702], by the UAMS Translational Research Institute [RR029884], and by an Arkansas Research Alliance Scholars Award to Peter A. Crooks. None of the funding sources participated in study design, in the collection, analysis and interpretation of data, in the writing of the report, or in the decision to submit the article for publication.

The studies described in this report were submitted in partial fulfillment of Benjamin M. Ford's doctoral dissertation: Ford BM (2017) Characterization of novel molecular scaffolds for cannabinoid receptor ligands: implications for drug development. Doctoral dissertation, University of Arkansas for Medical Sciences, Little Rock, AR.

13.0 Legends for Figures

Figure 1: *Panel A* – Effects of vehicle (open bar), 30 mg/kg Δ^9-THC (black bar), or 10 mg/kg rimonabant + Δ^9-THC (gray bar) on rectal temperature, measured in °C 60 min after injection. Bars represent group means, ±SEM. Asterisks indicate significant differences from vehicle ($p < 0.05$). *Panel B* – Time-activity curves for hypothermic effects of 30 mg/kg Δ^9-THC following the first (filled circles) and fifth daily injections (filled squares), and then again when tested after a 14 day drug abstinence (open circles) as measured in °C by radiotelemetry. Points represent group means, ±SEM, and any points without error bars indicate that the variability is contained within the point. Shaded area between dotted lines represents the range of core temperatures recorded over 24 hours following vehicle administration. *Panel C* – Lowest core temperatures recorded in °C following injection of vehicle or repeated daily administration of 30 mg/kg Δ^9-THC for 5 consecutive days, and then again after a 14 day drug abstinence period. Points represent group means, ±SEM, and any points without error bars indicate that the variability is contained within the point. Gray-filled point above the 'V' indicates mean lowest temperature recorded within 3 hours of vehicle administration. Asterisks indicate significant differences from vehicle, while hash marks indicate significant differences from Δ^9-THC Day 1 ($p < 0.05$). *Panel D* – Effects of vehicle (open bar), 100 mg/kg PNR-4-20 (black bar), or 10 mg/kg rimonabant + PNR-4-20 (gray bar) on rectal temperature, measured in °C 60 min after injection. All other graph properties as described in Panel A. *Panel E* – Time-activity curves for hypothermic effects of 100 mg/kg PNR-4-20 following the first (filled diamonds) and fifth daily injections (filled triangles), and then again when tested after a 14 day drug abstinence (open diamonds) as measured in °C by radiotelemetry. All other graph properties as described in Panel B. *Panel E* – Lowest core temperatures recorded in °C following injection of vehicle or repeated daily administration of 100 mg/kg PNR-4-20 for 5

consecutive days, and then again after a 14 day drug abstinence period. All other graph properties as described in Panel C.

Figure 2: *Panel A* – Effects of daily vehicle (open circles), 30 mg/kg Δ^9-THC (filled circles), 3 mg/kg JWH-018 (open triangles) or 100 mg/kg PNR-4-20 (open diamonds) on tail withdrawal latency from 50°C water across 5 days. For statistical comparisons, please see the Results section. All other graph properties as described in Figure 1. *Panel B* – Antinociceptive effects of vehicle, 30 mg/kg Δ^9-THC, 3 mg/kg JWH-018 or 100 mg/kg PNR-4-20 on the first administration (open bars) and on the final test administration after a 7 day abstinence period (filled bars.) Asterisks represent significant differences in tail withdrawal latency between day 1 and drug retest day after a 7 day abstinence period. All other graph properties as described in Figure 1.

Figure 3: Cataleptic effects of vehicle, 3 mg/kg JWH-018, 30 mg/kg Δ^9-THC, or 100 mg/kg PNR-4-20 assessed following the first daily injection (open bars), the fifth daily injection (gray bars), and following a retest after a 7-day drug abstinence period (black bars.) Asterisks represent catalepsy scores that differ significantly from those observed on day 1, for a given treatment condition. All other graph properties as described in Figure 1.

Figure 4: *Panel A* – Time-activity curves for hypothermic effects of 100 mg/kg PNR-4-20 following the first (filled diamonds) and fourth daily injections (open diamonds), and then for a cross-tolerance test with 30 mg/kg Δ^9-THC on day 5 (filled circles) as measured in °C by radiotelemetry. All other graph properties as described in Figure 1. *Panel B* – Lowest core temperatures recorded in °C following repeated daily administration of 100 mg/kg PNR-4-20 for 4 consecutive days (filled circles), and then for a cross-tolerance test with 30 mg/kg Δ^9-THC on day 5 (open square). Asterisks indicate significant differences from vehicle, while hash marks indicate significant differences from Day 1 ($p < 0.05$). All other graph properties as described in Figure 1. *Panel C* –

JPET Fast Forward. Published on March 4, 2019 as DOI: 10.1124/jpet.118.252965
This article has not been copyedited and formatted. The final version may differ from this version.

Time-activity curves for hypothermic effects of 30 mg/kg Δ^9-THC following the first (filled squares) and fourth daily injections (open squares), and then for a cross-tolerance test with 100 mg/kg PNR-4-20 on day 5 (filled circles) as measured in °C by radiotelemetry. All other graph properties as described in Figure 1. *Panel D* – Lowest core temperatures recorded in °C following repeated daily administration of 30 mg/kg Δ^9-THC for 4 consecutive days (filled squares), and then for a cross-tolerance test with 100 mg/kg PNR-4-20 on day 5 (open circle). Asterisks indicate significant differences from vehicle, while hash marks indicate significant differences from Day 1 ($p < 0.05$). All other graph properties as described in Figure 1.

Figure 5: Homologous binding curves for CP-55940 in hypothalamus (*Panel A*) or thalamus (*Panel B*) collected from mice previously treated with vehicle (filled circles), 30 mg/kg Δ^9-THC (open circles) or 100 mg/kg PNR-4-20 (open squares) once per day for 5 consecutive days. Points represent group means, ±SEM, and any points without error bars indicate that the variability is contained within the point. [^{3}H]-CP-55,940 homologous binding was used to determine Kd and B_{MAX} values reported in Table 3.

14.0 Tables

Table 1: ***Parameters of Δ^9-THC- and PNR-4-20-elicited hypothermia***

Day	30 mg/kg Δ^9-THC				100 mg/kg PNR-4-20			
	E_{MAX} (°C)	t_{MAX} (min)	AUC	N	E_{MAX} (°C)	t_{MAX} (min)	AUC	N
Vehicle	37.44 ± 0.31	-----	-----	5	37.21 ± 0.33	-----	-----	5
1	32.00 ± 0.25*	50	947	5	33.42 ± 0.56*	35	536	5
2	34.17 ± 0.51*	30	523	5	34.22 ± 0.47*	25	355	5
3	36.03 ± 0.56	55	185	5	36.29 ± 0.58	25	170	5
4	36.50 ± 0.64	280	59	5	35.56 ± 0.21*	25	241	5
5	36.14 ± 0.17	70	141	5	35.34 ± 0.39*	25	216	5
14-day drug abstinence period								
Retest	35.72 ± 0.40*	80	445	5	33.33 ± 0.54*	35	438	5

E_{MAX} values are presented as mean ± S.E.M of the lowest temperatures for each animal on each respective day and compound. t_{MAX} values indicate time in min when maximal hypothermic effects were observed for each respective day and compound. AUC represents area under the curve for each respective compound. Asterisks indicate E_{MAX} values which are significantly different from vehicle treated animals.

JPET Fast Forward. Published on March 4, 2019 as DOI: 10.1124/jpet.118.252965
This article has not been copyedited and formatted. The final version may differ from this version.

Table 2: ***Parameters of cross-tolerance between PNR-4-20 and Δ^9-THC***

Day	4-day 100 mg/kg PNR-4-20				Day	4-day 30 mg/kg Δ^9-THC			
	E_{MAX} (°C)	t_{MAX} (min)	AUC	N		E_{MAX} (°C)	t_{MAX} (min)	AUC	N
Vehicle	37.29 ± 0.33	-----	-----	5	**Vehicle**	37.29 ± 0.31	-----	-----	5
1	32.09 ± 0.19*	30	567	5	**1**	31.59 ± 0.17*	60	973	5
2	34.50 ± 0.95*	30	490	5	**2**	33.67 ± 0.32*	55	557	5
3	34.72 ± 0.57*	25	534	5	**3**	34.95 ± 0.28	50	362	5
4	34.26 ± 0.24*	35	492	5	**4**	34.97 ± 0.13	160	380	5
Δ^9-THC	33.98 ± 0.23*	125	865	5	**PNR-4-20**	34.62 ± 0.32	30	311	5

E_{MAX} values are presented as mean ± S.E.M of maximal hypothermic temperatures produced for each respective day and compound. t_{MAX} values indicate time in min when maximal hypothermic effects were observed for each respective day and compound. AUC represents area under the curve for each respective compound. Asterisks indicate E_{MAX} values which are significantly different from vehicle treated animals.

JPET Fast Forward. Published on March 4, 2019 as DOI: 10.1124/jpet.118.252965
This article has not been copyedited and formatted. The final version may differ from this version.

Table 3: ***Affinity and B_{MAX} values of hypothalamus and thalamus brain membranes in mice repeatedly treated with vehicle, Δ^9-THC, and PNR-4-20***

	[^{3}H]CP-55,940 Binding					
Treatment	**Kd (nM)**	**Kd (95% C.I.)**	**pKd (-Log[Kd])**	**B_{MAX} (pmole/mg)**	**B_{MAX} (95% C.I.)**	**N**
Hypothalamus						
Vehicle	0.77	0.29-2.45	9.12 ± 0.05[a]	0.96 ± 0.05[a]	0.47-1.26	4
Δ^9-THC	0.79	0.11-7.19	9.13 ± 0.08[a]	0.35 ± 0.16[b]	0.01-0.95	4
PNR-4-20	0.71	0.34-1.84	9.15 ± 0.04[a]	0.69 ± 0.04[c]	0.35-1.11	4
Thalamus						
Vehicle	0.83	0.40-1.76	9.14 ± 0.14[a]	1.15 ± 0.22[a]	0.59-1.63	4
Δ^9-THC	0.61	0.13-2.80	9.24 ± 0.11[a]	0.30 ± 0.05[b]	0.05-0.53	3
PNR-4-20	0.89	0.41-2.76	9.07 ± 0.08[a]	1.35 ± 0.11[a]	0.52-2.57	4

pKd and B_{MAX} values calculated from the homologous binding curves for CP-55940 in hypothalamus and thalamus are presented in Figure 6. Brain regions were collected from mice previously treated with vehicle (filled circles), 30 mg/kg Δ^9-THC (open circles) or 100 mg/kg PNR-4-20 (open squares) once per day for 5 consecutive days. The standard error of the mean for both Bmax and Kd values was derived from averaging the values of each curvefit for each replication, and these standard errors were used for the ANOVA. pKd and B_{MAX} values not sharing a letter are significantly different from each other, within each respective brain region; one-way ANOVA, Tukey's HSD *post-hoc* test.

JPET Fast Forward. Published on March 4, 2019 as DOI: 10.1124/jpet.118.252965
This article has not been copyedited and formatted. The final version may differ from this version.

15.0 Figures

FIGURE 1

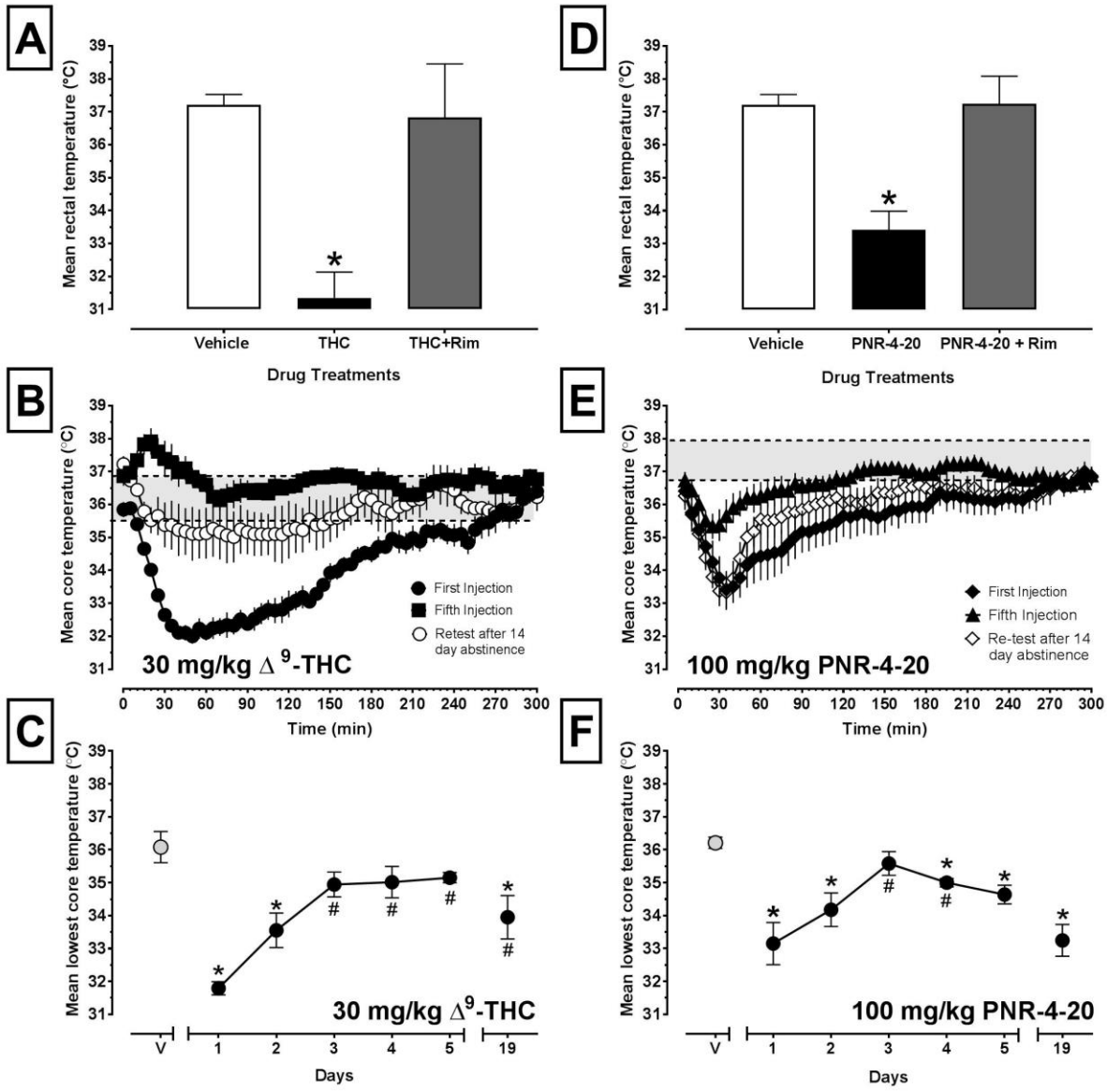

JPET Fast Forward. Published on March 4, 2019 as DOI: 10.1124/jpet.118.252965
This article has not been copyedited and formatted. The final version may differ from this version.

Figure 2

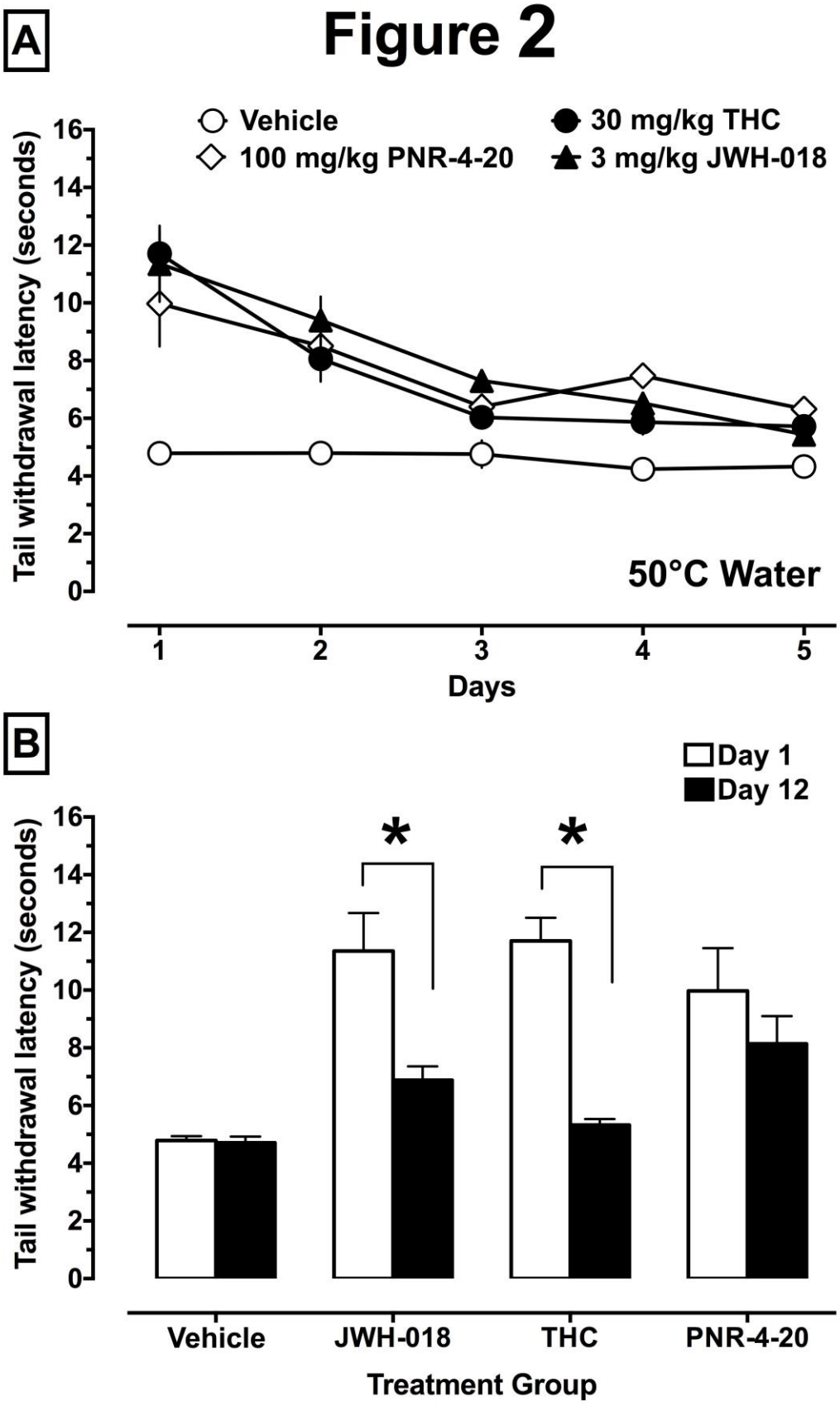

JPET Fast Forward. Published on March 4, 2019 as DOI: 10.1124/jpet.118.252965
This article has not been copyedited and formatted. The final version may differ from this version.

Figure 3

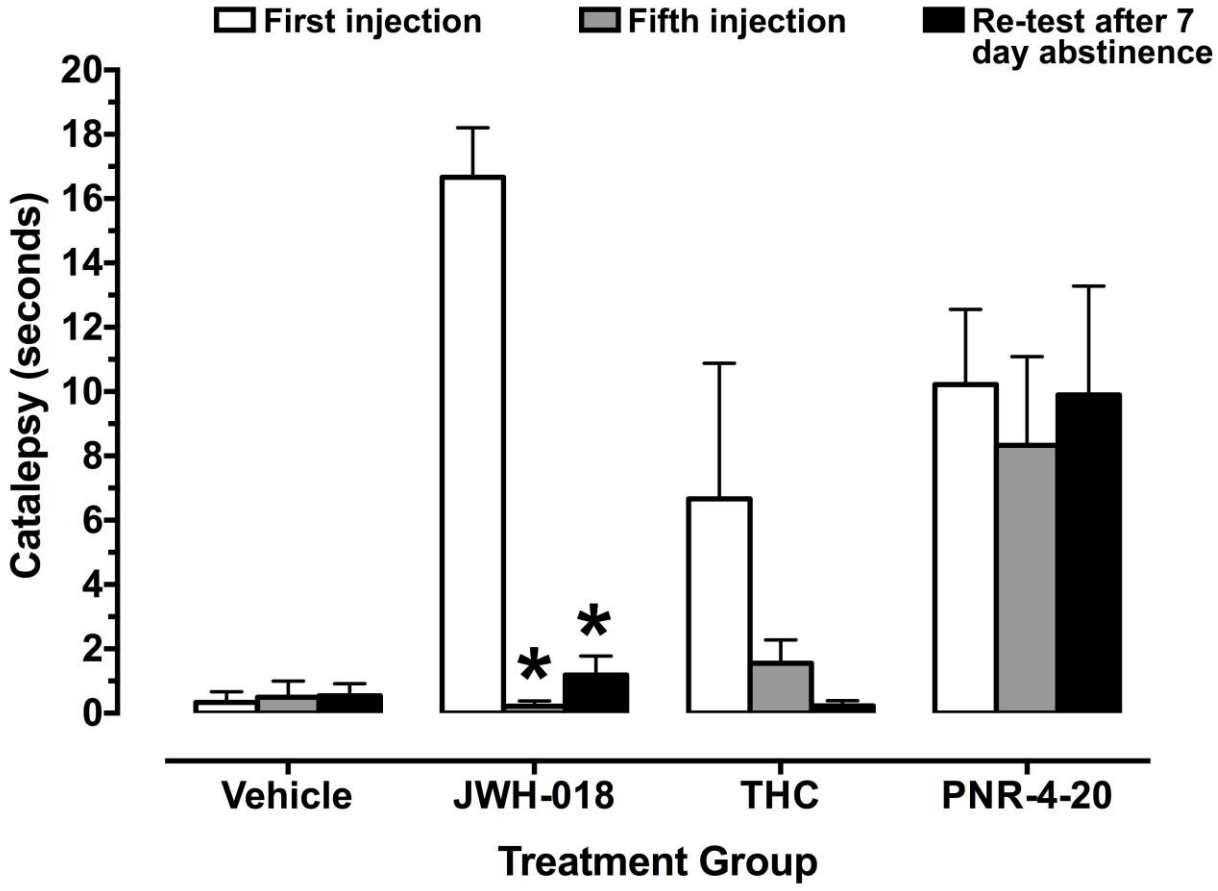

JPET Fast Forward. Published on March 4, 2019 as DOI: 10.1124/jpet.118.252965
This article has not been copyedited and formatted. The final version may differ from this version.

Figure 4

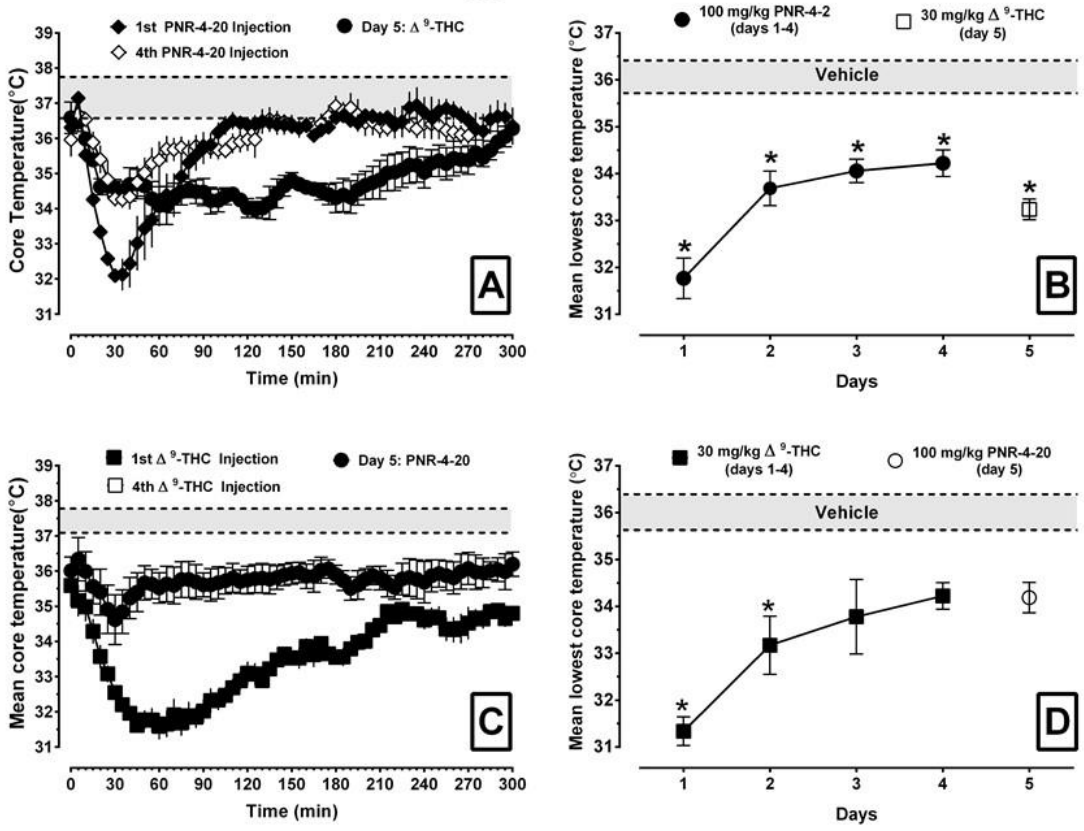

JPET Fast Forward. Published on March 4, 2019 as DOI: 10.1124/jpet.118.252965
This article has not been copyedited and formatted. The final version may differ from this version.

Figure 5